

**Role of the attractive forces in a supercooled liquid**Søren Toxvaerd *DNRF Center “Glass and Time,” IMFUFA, Department of Sciences, Roskilde University, Postbox 260, DK-4000 Roskilde, Denmark*

(Received 5 November 2020; accepted 4 February 2021; published 19 February 2021)

Molecular dynamics simulations of crystallization in a supercooled liquid of Lennard-Jones particles with different range of attractions shows that the inclusion of the attractive forces from the first, second, and third coordination shell increases the trend to crystallize systematic. The bond order  $Q_6$  in the supercooled liquid is heterogeneously distributed with clusters of particles with relative high bond order for a supercooled liquid, and a systematic increase of the extent of heterogeneity with increasing range of attractions. The onset of crystallization appears in such a cluster, which together explains the attractive forces influence on crystallization. The mean-square displacement and self-diffusion constant exhibit the same dependence on the range of attractions in the dynamics and shows, that the attractive forces and the range of the forces plays an important role for bond ordering, diffusion, and crystallization.

DOI: [10.1103/PhysRevE.103.022611](https://doi.org/10.1103/PhysRevE.103.022611)**I. INTRODUCTION**

Ever since Berni Alder [1] in 1957 performed the first molecular dynamics (MD) simulation of a hard sphere system with crystallization there has been a general understanding of, that crystallization of a simple liquid is given by the harsh repulsive short-range forces, and the MD simulation with particles with the more realistic Lennard-Jones (LJ) potential supported the assumption [2,3]. Not only did the thermodynamics of a LJ system agreed with the corresponding behavior of a system of noble gas atoms, but the tendency to crystallize for LJ systems with and without attractive forces is also very similar (Fig. 1). This similarity is explained with, that there is an overall agreement between the radial distribution function  $g(r)$  for LJ systems with- and without the attractive forces, as well as with the radial distribution function for a hard-sphere system. These rather closely similarities in the radial distributions of the particles have given reason to the well-established “perturbation theory” [4,5], where the thermodynamic and dynamic behavior of a system is obtained from systems of purely repulsive particles by mean-field corrections for contributions from the attractive forces.

Here we analyze the role of the attractive forces on the supercooled state and the crystallization by molecular dynamics (MD) simulations of LJ systems with different range of attractions. The simulations show, that the attractive forces play an important role in a supercooled liquid. They increase the bond order in the supercooled liquid, given by  $Q_6$  [6,7], and the tendency to crystallize.

**II. CRYSTALLIZATION OF THE SUPERCOOLED LIQUIDS**

The systems with different range of attractions are cooled down from the liquids at the state point  $(\rho_l, T_c) = (1.095, 2.25)$  for a liquid in equilibrium with fcc solid. The  $(\rho, T)$  phase diagrams for LJ systems with and without attractive

forces are shown in Fig. 1. The  $T(\rho)$  curves for coexisting liquids and fcc solids are obtained thermodynamically [8,9]. At  $(\rho_l, T_c) = (1.095, 2.25)$  a liquid with only repulsive forces and the LJ liquid with (full) attractions crystallize at the same state point.

The MD systems consist of  $N = 80\,000$  LJ particles, where the forces are “cutted and shifted” to zero at different particle distances greater than  $r_c$  [10]. The simulations (unit length  $l^* : \sigma$ ; unit time  $t^* : \sigma\sqrt{m/\epsilon}$ , for computational details see Ref. [10]) are performed for four different values of  $r_c$ : 3.5, 2.3, 1.41, and  $2^{1/6}$ , respectively. Only the strong repulsive LJ forces are included in the dynamics for the short cut at  $r_c = 2^{1/6}$ , and this system appears in the literature with the name WCA [5]. For  $r_c = 1.41$  also the attractive forces from particles in the first coordination shell are included, for  $r_c = 2.3$  the forces from the second coordination shell are included, and for  $r_c = 3.5$  the third shells forces are include in the dynamics.

There is a remarkably similarity between the LJ and the WCA system, which had led to to the perturbation expansion theories [4,5]. This is caused by the similarity in the radial distributions, and the inset shows the radial distribution function  $g(r)$  for the two systems in the supercooled state (red point in the figure). With red is  $g(r)$  for the supercooled liquid and the black points are  $g(r)$  for the WCA system. The blue curve in the inset is  $g(r)$  for a LJ fcc crystal and with blue points for fcc WCA. The  $g(r)$  for the WCA systems are shown with points for illustrative reasons because the differences between  $g(r)$  for LJ and WCA are small. The overall similarity between the two systems  $g(r)$  implies that the mean pair distributions in the supercooled state with coordination shells around a particles are almost identical for the two systems and that the mean effects of the attractive forces on pressure, energy, and free energy can be obtained as mean-field contributions.

The latent heat is released when a supercooled liquid crystallizes spontaneously, and the energy decreases and the

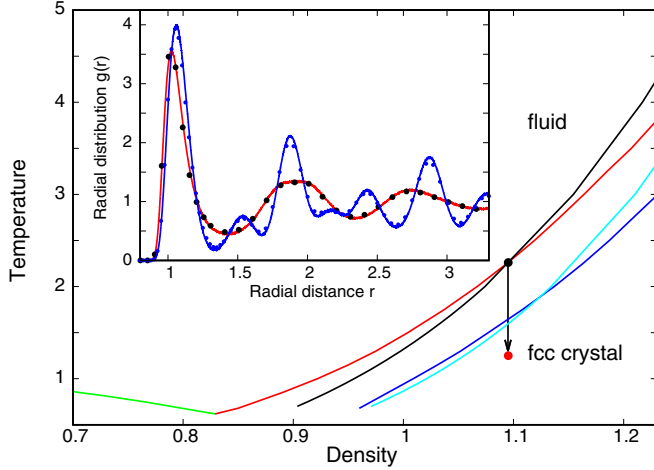


FIG. 1. The liquid-solid phase diagram for a LJ and a WCA system. LJ: green is liquid in equilibrium with gas; red: liquid in equilibrium with fcc solid; blue. WCA: black is fluid in equilibrium with fcc solid; light blue. The systems are cooled down from liquids at  $(\rho, T) = (1.095, 2.25)$ : black point to  $(\rho, T) = (1.095, 1.25)$ : red point. Inset: The radial distribution functions  $g(r)$  at  $(1.095, 1.25)$ . Red: Supercooled liquid, and with black points for WCA. Blue: fcc crystal and with blue points WCA.

temperature increases without a thermostat. In Ref. [11] the effect of a thermostat on the spontaneous crystallizations in the big MD supercooled systems was investigated by performing ensemble simulations with and without a thermostat and with the conclusion that the intensive MD thermostat, as expected, had no effect on the onset of crystallization. The present (NVT) simulations are with a thermostat by which the latent heat is removed smoothly, and the energy per particle decreases during the spontaneous crystallization at the constant supercooled temperature (Fig. 2).

The systems are cooled down from liquids at the state point where the liquids are in thermodynamic equilibrium with fcc solid, and at the point on the coexisting phase lines where the lines for the two systems crosses each other, by which the degree of supercooling  $T/T_c = 1.25/2.25 = 0.556$  at the constant density ( $\rho_l = 1.095$ ) is the same for the systems. The systems crystallize, however, with different tendency as can be seen in Fig. 2.

Figure 2 shows the log time evolution of the energies per particle for systems in the supercooled state and for different values of  $r_c$ . The mean-field energies from particles in the interval  $[r_c, 3.5]$  are added to the functions

$$u(t) = u(t, r_c) + 2\pi\rho \int_{r_c}^{3.5} g(r)u_{LJ}(r)r^2 dr, \quad (1)$$

and the energies  $u(t)$  for different cuts of the forces are almost equal before the onset of crystallization in accordance with the perturbation theory. The time evolution is shown with a logarithmic timescale. With black lines are the WCA systems with only repulsive forces, and they were simulated  $\Delta t = 22\,000$  ( $2.2 \times 10^7$  time steps). However, they remained in the supercooled state without crystallization. (The WCA systems were crystallized at a lower temperature  $T = 1.15$ .) The six blue curves denote  $r_c = 1.41$  with the attractive forces

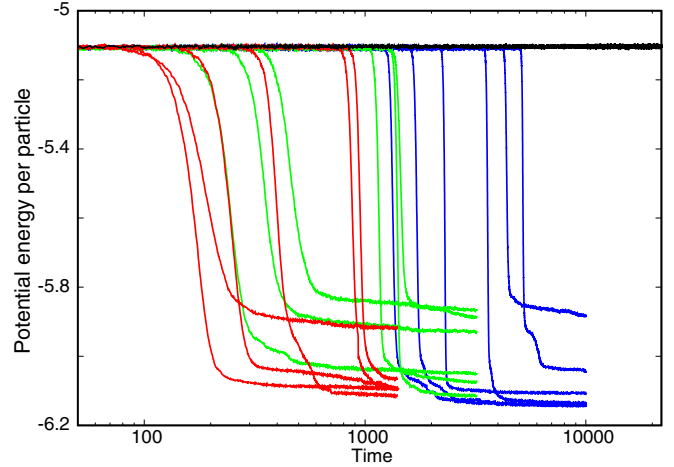


FIG. 2. Energy per particle as a function of log time after the quench to the supercooled state. Black lines denote the systems with only repulsive forces (WCA). The six blue curves denote  $r_c = 1.41$  (with the attractive forces in the first coordination shell included); six green curves denote  $r_c = 2.3$  (with attractive forces also from second coordination shell); six red curves denote  $r_c = 3.50$  (with attractive forces also from third coordination shell).

in the first coordination shell included in the force, and they crystallized within the time interval [1200, 5000] after the supercooling. The green curves denote  $r_c = 2.3$  with attractive forces also from the second coordination shell, and they crystallized within the time interval [150, 1300]. The red curves denote  $r_c = 3.50$  with attractive forces also from the third coordination shell, and they crystallized within the time interval [80, 850]. These data indicate a logarithmic effect of the attractive forces on the stability of a supercooled liquid. The effect of the attractive forces for  $3.5 < r_c$  on the stability of the supercooled state was, however, not investigated due to a lack of computer facilities for these very demanding simulations.

(The energies after the crystallization are rather different. In general a hard-sphere system as well as a LJ system crystallizes with polymorphism [12–14] to different polycrystalline fcc states with different mean energy per particles [11], as also seen in Fig. 2.)

The sensitivity of the range of attractions to the ability to crystallize is surprising given that the pair distributions of the different systems are very similar in the supercooled state as well as in the crystalline state. In the classical nucleation theory the size of the critical nucleus is the size, where the gain in free energy by an increase of particles in the crystal nucleus equals the cost of the increasing surface free energy, and these excess free energies should not be sensitive to the range of attractions due to the similarities in  $g(r)$ . But the distribution of bond order  $Q_6$  for the particles is sensitive to the range of the attractive forces.

A supercooled LJ liquid is characterized by a heterogeneous distribution of bond order, given by  $Q_6$  [11]. Here we will argue that it is the attractive forces impact on the extent of the heterogeneity of the bond order, which causes the difference in the tendency to crystallize. The distribution  $P(Q_6)$  of bond order  $Q_6(i)$  for the particles  $i$  in the LJ supercooled state is shown in Fig. 3 and with an inset, which shows

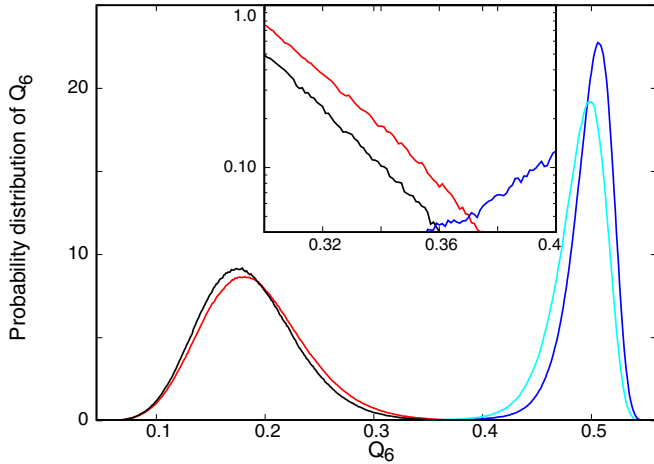


FIG. 3. Probability distribution  $P(Q_6)$  of bond order  $Q_6$  in the supercooled state. Red: LJ supercooled liquid with  $r_c = 3.5$ ; black: supercooled WCA fluid; blue: fcc LJ with  $r_c = 3.5$ ; light blue: WCA fcc. Inset:  $\log(P)$  in the interval  $Q_6 \in [0.30, 0.40]$ .

the log distributions in the bond-order interval for which the particles with these bond order are heterogeneous distributed. As in Ref. [11] there is an overlap in the distributions in supercooled liquid and in fcc crystal in this  $P(Q_6)$  interval  $Q_6 \in [0.35, 0.38]$ . In Ref. [11] we found that the particles with a relative high liquid bond order  $Q_6 > 0.25$  were heterogeneous distributed and with some particles with bond order  $Q_6 > 0.35$ . Furthermore, the critical crystal nucleus appeared in such a domain and with mean bond order  $\langle Q_6 \rangle \approx 0.38$ , which is significantly less than the bond order in the fcc crystal at the same state point.

The number of clusters with  $N$  particles with a bond order  $0.25 < Q_6$  are shown in the next figure. [A particle  $i$  in a cluster with  $Q_6(i) > 0.25$  is close to ( $r_{ij} < 1.41$ ) at least one other particle  $j$  in the cluster.] The distributions are obtained for the supercooled state as the mean of 200 independent determinations, and the inset shows the number of discrete and rare events of bigger clusters. The figure shows two things. For the first there is a crucial difference between the purely repulsive force system (WCA) and the systems with attractive forces which all exhibit big clusters with high liquid bond order. And, second, the inset shows that although the three distributions with different range of attractions looks pretty similar, there appears occasionally a much bigger clusters for the systems with long-range attractions.

The mean-bond order  $\langle Q_6 \rangle = 0.390$  in the critical nucleus is much less than in an ordered fcc crystal and the size of critical nuclei is the same for the three ranges of attractions. The extension of domains with relative high bond order varies, however, with the range of the cut (Fig. 4), and the critical nuclei appear in a domain with high bond order. So the extent of the heterogeneous distribution of high bond order in the supercooled liquid and thereby the probability to obtain a critical nucleus can explain the observed differences in the tendency to crystallize.

The critical nucleus were determined as described in Ref. [11]. Figure 5 shows a representative example of the time evolution of the number of particles  $N(t)$  in the biggest cluster,

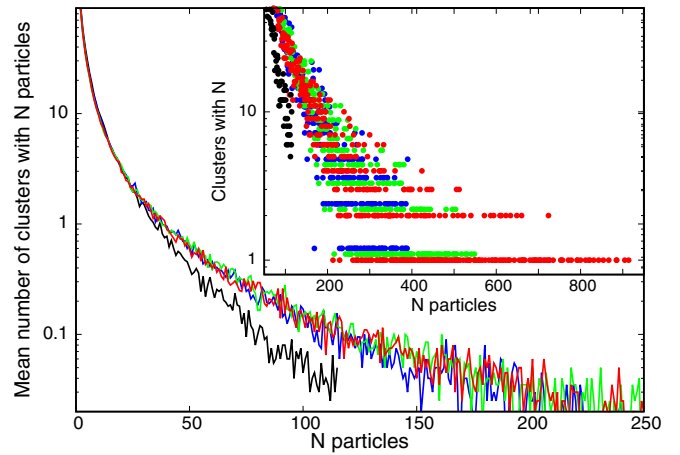


FIG. 4. Distributions (logarithmic) of clusters of  $N$  particles with  $Q_6 > 0.25$  in the supercooled LJ liquids. Red: The LJ system with  $r_c = 3.5$ ; green:  $r_c = 2.3$ ; blue:  $r_c = 1.41$ ; black:  $r_c = 2^{1/6}$  (WCA). Inset: The discrete distributions of big clusters (with points).

and with the mean bond order in the inset of the figure. The estimated critical sizes  $\langle N_c \rangle$  with the bond order  $\langle Q_6 \rangle$  for the simulations are as follows:

$$r_c = 1.41 : \langle N_c \rangle = 73 \pm 3 \text{ and } \langle Q_6 \rangle = 0.390 \pm 0.007$$

$$r_c = 2.30 : \langle N_c \rangle = 73 \pm 5 \text{ and } \langle Q_6 \rangle = 0.389 \pm 0.001$$

$$r_c = 3.50 : \langle N_c \rangle = 73 \pm 6 \text{ and } \langle Q_6 \rangle = 0.392 \pm 0.007.$$

The existence of “dynamic heterogeneity” in supercooled liquids have been known for a long time [15–17], and in Ref. [11] it was linked to the bonding in subdomains. If so, then the viscosity and particle diffusion should be different for domains with relative low bond order compared with subdomains with relative high bond order. This is, however,

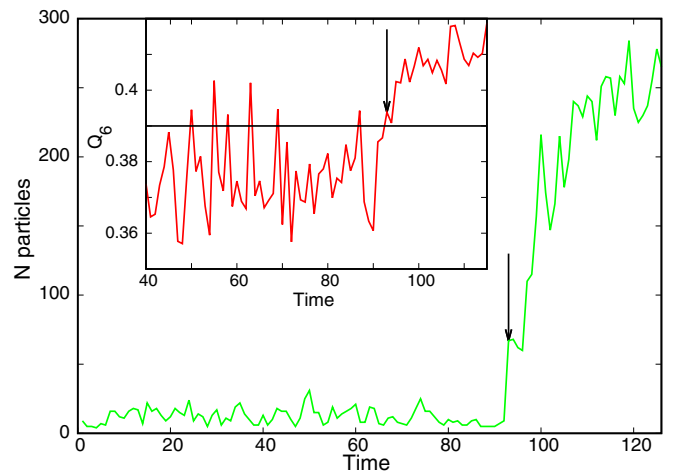


FIG. 5. An example of the number  $N(t)$  of particles in the biggest cluster of particles  $i$  with  $Q_6(i) > 0.25$ . The figure shows  $N(t)$  at the onset of crystallization for a system with  $r_c = 2.3$  (the green curve to the right in Fig. 2). The inset shows the mean bond order in the cluster. The arrows point to the time where the critical nucleus appears with  $N_c = 0.67$  and  $\langle Q_6 \rangle = 0.3938$ .

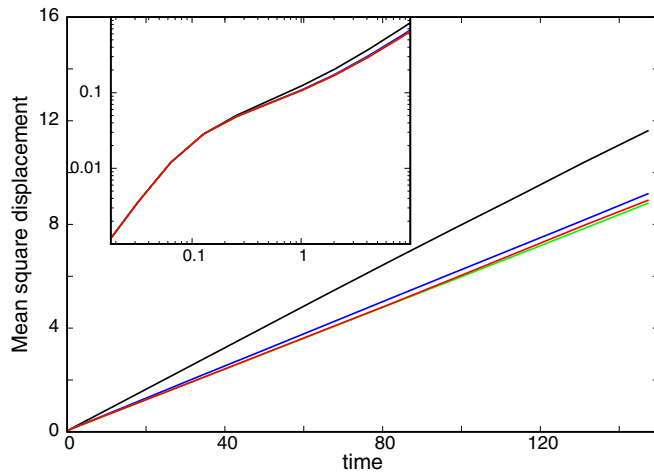


FIG. 6. Mean-square displacements at  $(T, \rho) = (1.25, 1.095)$ . Black:  $r_c = 2^{1/6}$ (WCA); blue:  $r_c = 1.41$ ; green:  $r_c = 2.3$ ; and red:  $r_c = 3.5$ , respectively. Inset: in logarithmic scales.

difficult to determine directly because the domains are not permanent and particles change bond order with time. But the overall particle diffusion reveals the differences and the main effect of the attractive forces on diffusion and viscosity. Figure 6 gives the mean-square displacements of a particle in the supercooled state and for different ranges of attractions. The figure shows that there is a difference in the slopes and thereby the self-diffusion constants  $D$  for the different range of attractions. The self-diffusion constants are WCA:  $D = 0.01315$ ;  $r_c = 1.41$ :  $D = 0.01033$ ;  $r_c = 2.30$ :  $D = 0.00991$ ;  $r_c = 3.5$ :  $D = 0.01004$ . The inset is the mean-square displacements in logarithmic scales, and it shows that the short-time “ballistic regime” is similar for all four systems and given by the strong repulsive forces. The behavior of the particle diffusion with respect to the range of the attractions can be explained by the fact that the domains with relative high bond order slow down the mobility of a particle in these domains, i.e., that the mobility is high in domains where the bond order is small and small in domains with relative high bond order, where the particles are tied together weakly.

The attractive forces dynamic effect in supercooled states has also been obtained for mixtures [18,19].

### III. CONCLUSION

In conclusion the radial distribution functions  $g(r)$  for the supercooled liquid as well as for the fcc solid are insensitive to the range of the attractions, and hence the free energies per particle (chemical potential) are also insensitive. Consistent with this observation, so is the size of the critical nuclei; but nonetheless, the tendency to crystallize depends on the range of attraction. The systems in the supercooled state exhibit, however, heterogeneous distributed particles with a relative high bond order for the supercooled state, and the extent of the heterogeneity is enhanced mainly from the attractions from the particles within the first coordination shell, but also the particles from the second and third coordination shells increase the number of domains with relative high bond order. In accordance with this observation, the systems crystallize much more easily for the systems with attractions and in a systematic way so that six crystallizations of particles with attractions from particles within three coordination shells crystallized  $\approx$ eight times faster than six systems with attractions only from the first coordination shell, whereas the systems with only repulsive forces did not crystallize at the supercooled state point.

This behavior of the heterogeneous bond-order distribution is consistent with the well-known “dynamic heterogeneity” in supercooled liquids, and the self-diffusion for the particles with different range of attractions supports the hypothesis. The attractions slow down the self-diffusion, the main effect comes from the attractions within the first coordination shell but also the longer-range attractions affect the diffusion. So in summary the attractive forces enhance the extent of the domains with high bond order, slow down the particle diffusion, and catalyze the crystallization. The sensitivity of the crystallization to the range of attractions makes it difficult to compare nucleation rates obtained by simulations with experimentally determined nucleation rates.

### ACKNOWLEDGMENT

This work was supported by the VILLUM Foundation’s Matter project Grant No. 16515.

- [1] B. J. Alder and T. E. Wainwright, *J. Chem. Phys.* **27**, 1208 (1957).
- [2] L. Verlet, *Phys. Rev.* **159**, 98 (1967).
- [3] J. P. Hansen and L. Verlet, *Phys. Rev.* **184**, 151 (1969).
- [4] J. A. Barker and D. Henderson, *J. Chem. Phys.* **47**, 4714 (1967).
- [5] J. Weeks, D. Chandler, and H. C. Andersen, *J. Chem. Phys.* **54**, 5237 (1971).
- [6] P. J. Steinhardt, D. R. Nelson, and M. Ronchetti, *Phys. Rev. B* **28**, 784 (1983).
- [7] W. Lechner and C. Dellago, *J. Chem. Phys.* **129**, 114707 (2008).
- [8] A. Ahmed and R. J. Sadus, *Phys. Rev. E* **80**, 061101 (2009).
- [9] M. A. Barroso and A. L. Ferreira, *J. Chem. Phys.* **116**, 7145 (2002).
- [10] S. Toxvaerd and J. C. Dyre, *J. Chem. Phys.* **134**, 081102 (2011).
- [11] S. Toxvaerd, *Eur. Phys. J. B* **93**, 202 (2020).
- [12] B. O’Malley and I. Snook, *Phys. Rev. Lett.* **90**, 085702 (2003).
- [13] C. Desgranges and J. Delhommelle, *Phys. Rev. Lett.* **98**, 235502 (2007).
- [14] C. Desgranges and J. Delhommelle, *J. Phys. Chem. B* **111**, 1465 (2007).
- [15] M. D. Ediger, *Annu. Rev. Phys. Chem.* **51**, 99 (2000).
- [16] A. Widmer-Cooper, P. Harrowell, and H. Fynewever, *Phys. Rev. Lett.* **93**, 135701 (2004).
- [17] A. Widmer-Cooper and P. Harrowell, *Phys. Rev. Lett.* **96**, 185701 (2006).
- [18] L. Berthier and G. Tarjus, *J. Chem. Phys.* **134**, 214503 (2011).
- [19] S. Toxvaerd and J. C. Dyre, *J. Chem. Phys.* **135**, 134501 (2011).